Energy Levels of Dy^{165}†

R. K. SHELINE AND W. N. SHELTON
Florida State University, Tallahassee, Florida

H. T. MOTZ AND R. E. CARTER
Los Alamos Scientific Laboratory, Los Alamos, New Mexico

(Received 15 June 1964)

Eighty levels which have been observed in Dy^{165} utilizing the reaction $Dy^{164}(d,p)Dy^{165}$ with 12-MeV deuterons are reported. The ground-state Q for the reaction was determined as 3488±5 keV. Thermal neutron capture gamma rays from a sample of natural dysprosium have been measured over the energy range of 900 to 6000 keV. The neutron binding energy of Dy^{165} is determined to be 5715±4 keV. These complimentary methods are a considerable aid in analysis, because the observed intensities permit spin assignments for (a) those levels populated by the strong high-energy capture gamma rays and (b) several of the (d,p)-populated levels. The analysis suggests the following spectroscopic interpretation (band head energies, keV, in parentheses; Nilsson asymptotic quantum numbers in brackets): (ground state), $\frac{7}{2}+[633]$ with superimposed rotational to 13/2+; (108.16), $\frac{1}{2}-[521]$ rotational band to 11/2−; (184), $\frac{5}{2}-[512]$ rotational band to 11/2−; (∼535), $\frac{5}{2}-[523]$ rotational band to $\frac{9}{2}-$; (539), $\frac{3}{2}+\gamma$ band built on $\frac{7}{2}+[633]$ with rotational members to $\frac{9}{2}+$; (574), $\frac{3}{2}-\gamma$ band on $\frac{1}{2}-[521]$ with rotational members to $\frac{7}{2}-$; and (606), $\frac{3}{2}-[521]$? rotational band to $\frac{5}{2}-$. The gamma vibrational bands are the first postulated on odd-neutron intrinsic Nilsson orbitals. An analysis is made of the K-2 gamma bands of odd-A nuclei. Their energy systematics is found to mirror closely that of the gamma bands of neighboring even–even nuclei.

I. INTRODUCTION

THE nucleus Dy^{165} should be a typical odd-A deformed nucleus. However, little is known about its level structure except for two states[1,2] resulting from the isomerism of Dy^{165}. These are a 75-sec isomeric state at[3] 108.16 keV and the 2.3-h ground state. The ground-state spin of Dy^{165} has been measured[4] to be $\frac{7}{2}$. This measured spin, together with the systematics of other 99 neutron species and the branching ratios in the decay of Dy^{165} into Ho^{165}, strongly suggests the assignment $\frac{7}{2}+[633]$ for the ground state. Since the 108.16-keV isomeric transition has been shown to have $E3$ character,[5] the level at 108.16 keV probably has spin-parity $\frac{1}{2}-$ or $\frac{3}{2}-$. The description in terms of the $\frac{1}{2}-[521]$ state follows naturally from the systematics of the first excited states in other 99 neutron species (Er^{167} and Yb^{169}) and the systematics of the ground states in 101 neutron species (Yb^{171} and Hf^{173}). The Nilsson level scheme inverts the order but indicates the presence of the $\frac{7}{2}+[633]$ and $\frac{1}{2}-[521]$ states. The 1.2-min state and published neutron capture results will be discussed in Sec. II.B.

This research also afforded the opportunity to study vibrational states in odd-A nuclei. Since the first observation of a vibrational state in an odd-A deformed nucleus,[6] an increasing number of these excitations has been observed.[7–11] However, the γ vibration has been built on an intrinsic state of a proton orbital in all previously studied cases. The observation in this research of γ vibrations built on neutron orbitals is of considerable interest. Systematics of vibrational states in deformed odd-A nuclei are also presented.

Two complimentary methods have been utilized to study the levels in Dy^{165}. Thermal neutron capture in Dy^{164} leads to a compound state in Dy^{165} having spin-parity $\frac{1}{2}+$. Dipole transitions from this compound state excite only spin-parity $\frac{1}{2}\pm$ and $\frac{3}{2}\pm$ low-lying states. The states populated by the stronger high-energy transitions from neutron capture thus consist of a restricted set of low spin states. The (d,p) reaction, on the other hand, should populate almost all one-quasiparticle states. This research has as its aim then, not only a more thorough understanding of the levels and spectroscopy of Dy^{165}, but also an evaluation of the complimentarity of these two experimental methods.

II. EXPERIMENTAL METHODS AND RESULTS

A. $Dy^{164}(d,p)Dy^{165}$ Reaction Spectroscopy

The reaction $Dy^{164}(d,p)Dy^{165}$ has been studied with 12.0-MeV deuterons using the Florida State University tandem Van de Graaff. The deuteron beam was focused through a series of slits collimating it to a

† Work supported by the U. S. Atomic Energy Commission.

[1] B. R. Mottelson and S. G. Nilsson, Kgl. Danske Videnskab. Selskab. Mat. Fys. Skrifter **1**, No. 8 (1959).

[2] B. Harmatz, T. H. Handley, and J. W. Mihelich, Phys. Rev. **128**, 1186 (1962).

[3] R. Hardell and S. Nilsson, Nucl. Phys. **39**, 286 (1962).

[4] A. Y. Cabezas, I. Lindgren, and R. Marrus, Phys. Rev. **122**, 1796 (1961).

[5] W. C. Jordan, J. M. Cork, and S. B. Burson, Phys. Rev. **92**, 1218 (1953).

[6] F. P. Cranston, M. E. Bunker, and J. W. Starner, Bull. Am. Phys. Soc. **5**, 255 (1960); and private communication, 1959.

[7] C. J. Gallagher, Jr., W. F. Edwards, and G. Manning, Nucl. Phys. **19**, 18 (1960).

[8] O. Nathan and V. I. Popov, Nucl. Phys. **21**, 631 (1960).

[9] J. Valentin, D. J. Horen, and J. M. Hollander, Nucl. Phys. **31**, 353 (1962).

[10] R. M. Diamond, B. Elbek, and F. S. Stephens, Nucl. Phys. **43**, 560 (1963).

[11] J. S. Greenberg, D. A. Bromley, E. Bishop, and G. Seaman, in *Direct Interactions and Nuclear Reaction Mechanisms*, edited by E. Clementel and C. Villi (Gordon and Breach Publishers Inc., New York, 1963), p. 941.

$\frac{1}{4}\times$3-mm spot on the target, which served as a line source for the magnetic spectrograph. Beam currents ranged from 0.3 to 0.6 μA through the slits.

Targets of the separated Dy^{164}, 90%; Dy^{163}, 7.8%; Dy^{162}, 1.8%; Dy^{161}, 0.4% obtained from the Stable Isotopes Division at Oak Ridge were prepared in the

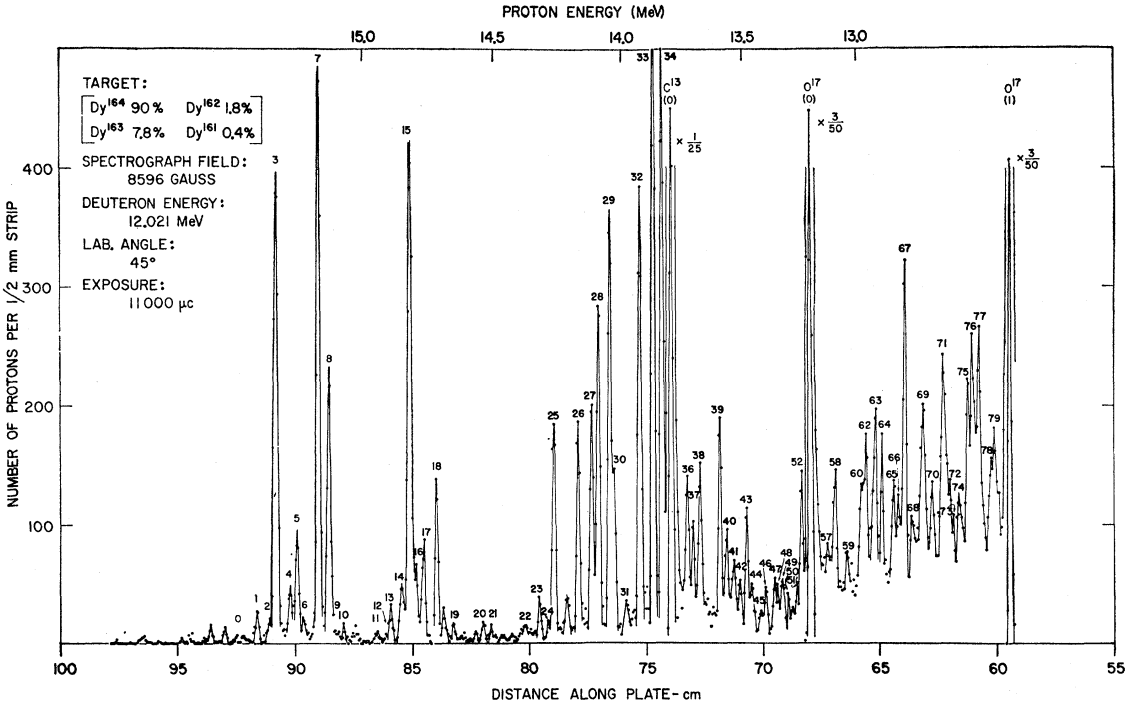

FIG. 1. Proton spectrum from the reaction Dy(d,p)Dy observed at 45°.

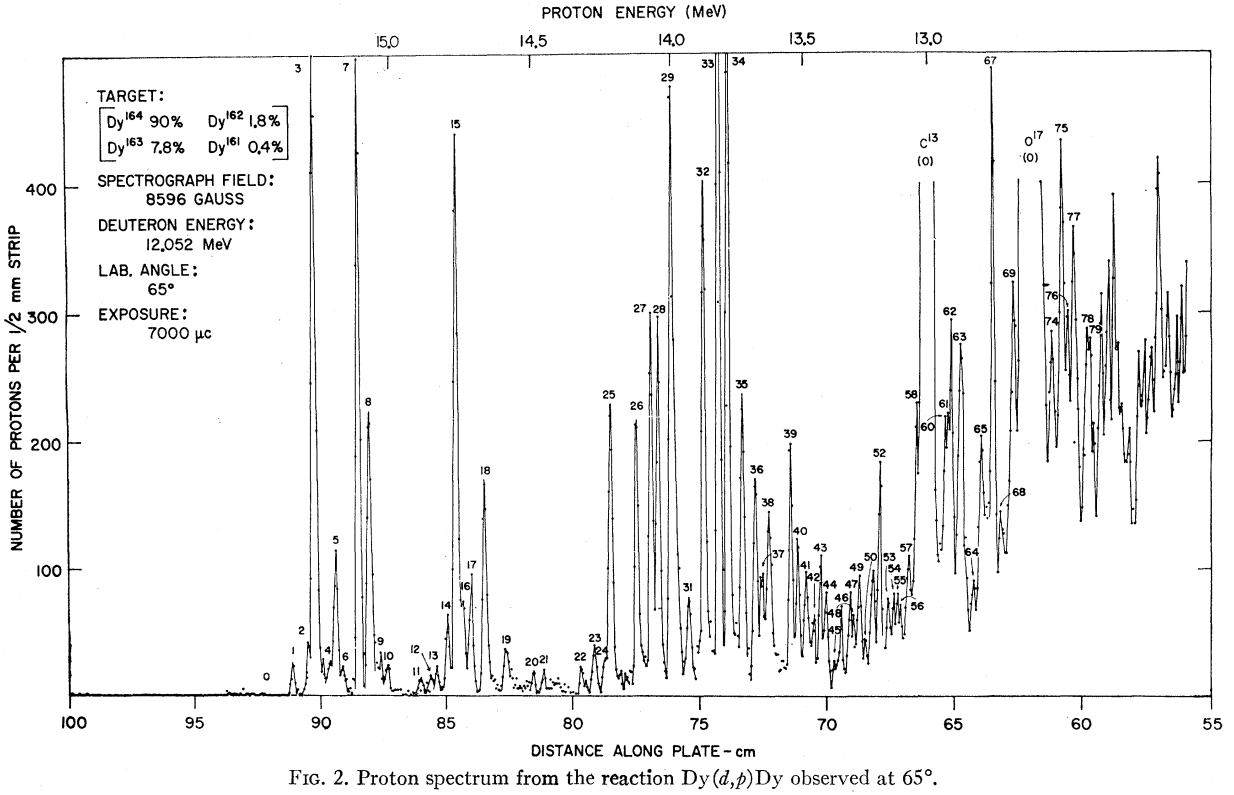

FIG. 2. Proton spectrum from the reaction Dy(d,p)Dy observed at 65°.

TABLE I. Levels in Dy^{165} from the (d,p) reaction.

Group number	Q (keV)	Excitation (keV)	$Dy^{163}(d,p)Dy^{164}$ contribution	Group number	Q (keV)	Excitation (keV)	$Dy^{163}(d,p)Dy^{164}$ contribution
0	3488[a]	0		41	1595	1893	
1	3451	...	~100%	42	1568	1920	
2	3404	84.5		43	1539	1949	
3	3380	108.2	~5%	44	1517	1971	
4	3330	158.4		45	1482	2006	
5	3307	180.7	~10%				
				46	1459	2029	
6	3281	...	~100%	47	1419	2069	
7	3226	261.5	~4%	48	1412	2076	
8*A*	3192	296.3		49	1390	2098	
8*B*	3185	303.3		50	1364	2124	
9	(3151)	(336.9)[b]					
10	3128	360.5	~25%	51	1336	2152	
				52	1309	2179	
11	(3008)	(480)[b]		53	1279	2209	
12	(2969)	(519)[b]		54	1258	2230	
13	2951	537[c]		55	1241	2247	
14	2914	574[c]					
15	2883	605		56	1220	2268	
				57	1200	2288	
16	2859	629	~3%	58	1165	2323	
17	2830	658		59	1115	2373	
18	2781	707	~10%	60	1056	2432	
19	2715	773					
20	2604	884	~40%	61	1043	2445	
				62	1029	2459	
21	2569	919		63	993	2495	
22	2434	1054		64	964	2524	
23	2382	1106	<5%	65	912	2576	
24	2343	1145					
25	2322	1166		66	892	2596	
				67	868	2620	
26	2226	1262		68	831	2657	
27	2172	1316		69	784	2704	
28	2145	1343		70	747	2741	
29	2099	1389					
30	2181	1407		71	696	2792	
				72	673	2815	
31	2036	1452		73	654	2834	
32	1982	1506[d]		74	629	2859	
33	1925	1563		75	589	2899	
34	1888	1598					
35	1836	1652		76	568	2920	
				77	540	2948	
36	1788	1700		78	482	3006	
37	1763	1725		79	472	3016	
38	1735	1753					
39	1653	1835					
40	1625	1863					

[a] Proton group not observed: Q calculated from 108.2-keV reference level.
[b] Group uncertain: energy not well determined.
[c] Group assumed to be a doublet.
[d] $Dy^{163}(d,p)Dy^{164}$ spectrum too dense to analyze at higher excitations.

following manner. Carbon was deposited on glass microscope slides which had previously been coated with Teepol by vacuum evaporation. The Dy^{164} as oxide was then evaporated onto the carbon by electron bombardment heating a carbon crucible containing the oxide. The carbon film containing the Dy^{164} target was then floated off in ion-exchanged water and picked up on an Al frame having an area of 0.8 cm^2 designed to fit the target chamber. Thicknesses of carbon backings were 15–30 $\mu g/cm^2$, whereas the $(Dy^{164})_2O_3$ targets were 100–200 $\mu g/cm^2$ thick.

The protons emitted from the (d,p) reaction were analyzed in a modified Browne-Buechner broad-range magnetic spectrograph.[12] More complete details of the spectrograph are contained elsewhere.[13] Proton groups from the (d,p) reaction are bent toward an array of four 2-in.×10-in. 50-μ emulsion Kodak plates. These plates are arranged end to end and are spring locked against the focal surface of the magnet. During these experiments the emulsions were covered with 5-mil Al foil to stop the deuterons and simplify the tedious job of plate

[12] C. P. Browne and W. W. Buechner, Rev. Sci. Instr. **27**, 899 (1956).
[13] W. Neil Shelton, thesis submitted to Florida State University, 1962 (unpublished).

TABLE II. $Dy^{164}(d,p)Dy^{165}$ least-squares results for 60° data.

Number	Excitation	Intensity
2	85.0 ±1.0	6.5± 0.8
3[a]	108.16±0.2	99.0± 2.6
4	159.1 ±1.4	4.9± 0.7
5	181.1 ±0.5	20.7± 1.2
7	262.3 ±0.3	91. ± 3.0
8*A*	296.3 ±2.5	24. ±10.
8*B*	303.3 ±3.8	24. ±10.
9	336.9 ±2.5	3.5± 0.9
10	360.5 ±1.2	4.2± 0.6

[a] Reference level.

counting. Plate counting is accomplished after development with precision stage microscopes having dark-field illumination. Data are taken and presented as proton tracks per ½-mm strip of plate as a function of distance along the plate array. A program utilizing the Florida State University 709 computer allows the conversion of plate distance into proton energy. The acceptance solid angle of the spectrograph was set at 1.78×10^{-4} sr. At this solid angle the resolution of the spectrograph (full width at half-maximum) was ~12 keV over the region of interest. This corresponds for 15-MeV protons (toward the upper energy of protons emitted in these experiments) to ~0.08% resolution. Actual proton-energy determination can be made more accurately than 10 keV. Energy differences which are our main interest here are often quoted to ±1 keV although this is obviously a function of the statistical accuracy of the proton group under consideration.

The protons resulting from the reaction $Dy^{164}(d,p)Dy^{165}$ using 12.0-MeV deuterons were analyzed at 45 and 65° with respect to the incident beam. These spectra are shown in Figs. 1 and 2, respectively. Table I lists all the immediately obvious proton groups ascribed to dysprosium in Figs. 1 and 2 together with the Q, in keV, for the levels, the excitation in Dy^{165}, and an explanation of isotopic impurities. A number of comments are in order about the lower energy part of the spectrum. (1) As will be shown later, the $\frac{7}{2}+$ ground state of Dy^{165} is not appreciably populated in the (d,p) reaction. However, the $\frac{1}{2}-$ state at 108.16 keV is strongly populated (peak 3). The Q value is 3380 keV. Consequently, the $Dy^{164}(d,p)Dy^{165}$ Q value to the ground state is 3380+108 or 3488±5 keV. (2) The group numbered "1" results from the 7.8% Dy^{163} present in the target and corresponds to the 1987-keV state[14] in Dy^{164}. (3) The group numbered "6" is due entirely to the 2158-keV state in Dy^{164}, (4) Several of the "real" Dy^{165} groups have some contamination of Dy^{164} groups in them as indicated in Table I. The comparison of these data with the (n,γ) data and their interpretation in terms of rotational bands built on the appropriate Nilsson intrinsic states will be considered in Sec. III.

During the process of this research, it was recognized that energy differences, which were previously estimated from differences in the ⅓ height of the leading edges of two proton peaks, could be determined with considerably greater accuracy. This is accomplished by the application of a least-squares curve-fitting program which determines the centroids of the proton groups and, at the same time, determines the uncertainty in the centroid assignment. As an example of the accuracy possible, the computed results for those peaks from the 60° data assigned to $Dy^{164}(d,p)Dy^{165}$ between 84- and 360-keV excitation are given in Table II. It is particularly important to notice that not only are the energies more accurately determined [see comparison with high-energy (n,γ) transitions, Sec. II.C] but also in one case (peak 8) a doublet which would probably otherwise have been missed is fitted by the least-squares program.

B. $Dy^{164}(n,\gamma)Dy^{165}$

Low-energy transitions in $Dy^{164}(n,\gamma)Dy^{165}$ were first observed by Hibdon and Muelhause[15] using a permanent magnet spectrograph to detect conversion electrons. They found transitions of approximately 82, 106, and 189 keV whose multipolarity was judged to be M1 or *E*1, *E*3, and *E*2 or *M*2. Several experimenters[16–18] have used scintillation spectrometers and are in general agreement that three dominant gamma rays of approximate energies and intensities 80 keV (15%), 105 keV (50%), and 185 keV (20%) are present in a very complex spectrum. These intensities are derived after correcting for internal conversion associated with *M*1, *E*3, and *E*1 transitions. Jurney has observed[19] these three transitions and finds corrected intensities of 19%, 53%, and 27% with a ±30% absolute error. These values must be regarded as upper limits since more than one gamma-ray intensity is integrated.

The crystal-diffraction spectrometer constructed by the Munich group at Risø has reported some 200 gamma rays from $Dy^{164}(n,\gamma)Dy^{165}$ in equilibrium with its decay products from 29 to 1260 keV.[20] The accuracy of these observations is extremely high, having errors of one to several hundred electron volts ascribed to them. There are three strong transitions which are believed to be Dy^{165} radiations and to correspond to the three above-listed transitions. They are 83.397, 108.160, and 184.255

[14] The values quoted here ascribed to the residual nucleus Dy^{164} are from low isotopic content of Dy^{163} and are not as accurate as those quoted by W. N. Shelton and R. K. Sheline, Phys. Rev. 133, B624 (1964).

[15] C. T. Hibdon and C. O. Muelhause, Phys. Rev. 88, 943 (1952).

[16] V. L. Sklyarevskii, E. P. Stepanov, and B. A. Obinyakov, At. Energ. (USSR) 4, 22 (1958) [English transl.: Soviet J. Atomic Energy 4, 19 (1958)].

[17] J. E. Draper, Phys. Rev. 114, 268 (1959).

[18] R. C. Greenwood, Armour Research Foundation Report No. ARF 1193-6 (unpublished).

[19] E. T. Jurney (private communication, 1963).

[20] O. W. B. Schult, B. P. Maier, and U. Gruber (private communication, 1963); Z. Physik (to be published).

keV. It can be immediately seen that within their errors of 4, 3, and 5 eV, these three transitions could not form a stopover-crossover set as originally thought from the less accurate data of Hibdon and Muelhause. The second transition is known to correspond to the known 1.2-min isomeric state; the others will be assigned later in this paper.

High-energy observations of gamma radiation from capture in natural dysprosium have been reported by Groshev *et al.*[21] and by Motz and Carter.[22] The former work will not be listed here since it is of inferior resolution, which is incapable of showing sufficient detail. The latter work has been repeated and averaged with more recent results to be reported in this paper. A summary of these results was presented at a topical meeting of the American Physical Society in 1963.[23]

The thermal-neutron-absorption cross section of Dy^{164} is about 2500 b and accounts for 77% of the total thermal-neutron absorption in natural dysprosium. Dy^{161} accounts for approximately 12% of the thermal absorption and the remaining 10% is divided between Dy^{162} and Dy^{163}. The population of the 1.2-min isomeric state in Dy^{165} is reported to be 65% of the total cross section[24] of Dy^{164}. For this work, 17 g of natural Dy_2O_3 in the form of 14 cylinders each $\frac{1}{8}$ in. in diameter and 3 in. long were packed into a graphite block to form the source. The gamma-ray spectrum was obtained using the Compton spectrometer at the OWR reactor in Los Alamos.[22,25] The source material was placed in the graphite thermal column of the reactor and a collimator allows a gamma-ray beam to emerge through the shield. The gamma-ray channel is arranged so that background from the reactor core region is minimized. The three well-known gamma rays from $C^{12}(n,\gamma)C^{13}$ are present in all spectra due to neutron capture in the graphite.

Coincidences between Compton electrons detected in the focal plane of a double-focusing magnetic spectrometer and back-scattered gamma rays are recorded. Four electron detectors and two gamma-ray detectors are used and coincidences are detected by a 4×2 coincidence matrix. A 12.4 mg/cm² beryllium radiator 3 mm wide and 50 mm high was used to obtain the dysprosium data shown in Fig. 3. Gamma-ray energies are computed as a function of the electron momentum and the average gamma-ray scattering angle for each pair of detectors. A rotating coil system controls the magnetic field using

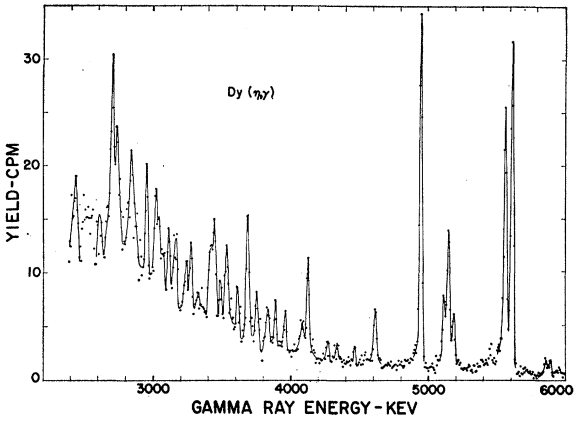

FIG. 3. High-energy gamma-ray spectrum from thermal neutron irradiation of natural dysprosium. The lines at 3683 and 4944 keV are from the $C^{12}(n,\gamma)C^{13}$ reaction in the graphite moderator of the thermal column.

a temperature-regulated permanent magnet as a reference field.

The linearity of the system has been studied by measurements of the spectra of $Be^9(n,\gamma)Be^{10}$ and $N^{14}(n,\gamma)N^{15}$. Gamma rays from these reactions, which involve crossover and stopover transitions from 1 to 10.8 MeV, must be consistent when a small correction for nuclear recoil is included. These measurements indicate that the linearity is good to within two parts in 10^4 over this energy region and thus a one-point energy calibration is sufficient. A reactor-activated source of Na^{24} is used for this purpose and the 2753.98±0.25-keV gamma ray[26] is used as a reference line.

The energies of the observed lines are obtained by fitting a skewed Gaussian function to the accumulated coincidence versus energy data. This computation allows as many as 14 lines to be fitted at once with independent control of most parameters. Errors associated with energy differences between lines can usually be taken from the standard deviations of the fitted values when data are obtained on the same magnet cycle with acceptable stability of operation. These standard deviations vary from 0.2 keV to about 4 keV depending upon the statistical accuracy. Systematic errors involving calibration and nonlinearity enter into the over-all error and amount to less than one part in 10^3. The energy differences are the most significant quantity, however, in determining the low-lying level positions.

Some of the data were taken in 1960, but most of the results quoted here were obtained in 1962 and are tabulated in Table III. It is important to realize that the standard deviations quoted in Table III are determined from the least-squares fitting, assuming the spectrum to consist of only those lines listed. If, for example, it can be shown that a peak which is assumed

[21] L. V. Groshev, A. M. Demidov, V. N. Lutsenko, and V. I. Pelekhov, At. Energ. (USSR) 4, 5 (1958) [English transl.: Soviet J. Atomic Energy 4, 1 (1958)]; J. Nucl. Energy 8, 50 (1958).

[22] H. T. Motz and R. E. Carter, Proceedings of the International Conference on Nuclidic Masses, Hamilton, 1960 (University of Toronto Press, Toronto, 1960).

[23] H. T. Motz and R. E. Carter, Argonne National Laboratory Report ANL-6797 (unpublished).

[24] R. Sher, S. Tassan, E. Weinstock, and A. Hellsten, Nucl. Sci. Eng. **11**, 369–376 (1961).

[25] H. T. Motz, R. E. Carter, and W. D. Barfield, in *Proceedings of the Symposium, Vienna, 1960* (I.A.E.A., Vienna, 1962), pp. 225–238.

[26] G. Murray, R. Graham, J. Geiger, and G. Ewan, Chalk River PRP 49, AECL, Ltd., 31 January–31 March 1961, also AECL-1266 (unpublished).

TABLE III. Neutron-capture gamma rays from natural dysprosium.[a]

Line number[b]	E_γ	$\pm\delta E_\gamma$	I	$\pm\delta I$	Class[c]
	5881.5	2	18	3	*B*
	5850.0	1	22	3	*B*
	5725.4	4	6	2.5	*B*
	5671.7	4	8	3	*B*
3′	5606.7	0.2	663[d]	12	*A*
4′	5556.4	0.3	485[e]	12	*A*
	5526	3	30	8	*B*
	5453	3	17	5	*B*
	5211	7	7	5	*C*
13′	5175.4	1.0	88[f]	8	*A*
14′	5142.6	0.5	253[g]	8	*A*
15′	5108.9	0.8	108[h]	8	*A*
	4944.0	0.2	626	12	*D*
23′	4612.3	0.6	103	7	*A*
25′	4547	3	18	5	*A*
	4460.4	2	23	5	*A*
	4419	4	11	4	*C*
	4344.7	2	17	3	*A*
	4317.4	1	32	3	*A*
	4282	4	10	4	*A*
31″	4263	3	20	4	*A*
	4246	3	18	5	*A*
33′	4156	2	23	4	*A*
	4123.2	0.4	171	8	*A*
	4091	2	37	7	*A*
	4072.4	1	70	8	*A*
	4030	4	21	6	*A*
36′	4018	3	25	7	*A*
38′	3956.9	1	73	9	*A*
	3923	3	23	7	*A*
39′	3885.2	1	70	8	*A*
	3841	1	60	10	*A*
41′	3820	2	40	7	*A*
44′	3748	2	48	7	*A*
45′	3708	3	27	7	*A*
	3683.4	1	182	10	*D*
	3627	6	18	11	*C*
49′	3613	3	41	13	*A*
51′	3552	2	52	8	*A*
52′	3526.6	1	89	10	*A*
53′	3501	3	36	10	*A*
54′	3482	2	62	10	*A*
56′	3441	1	194	6	*A*
57′	3421	2	120	6	*A*
	3408	2	84	16	*A*
58′	3392	4	28	10	*A*
	3352	3	48	12	*A*
	3317	2	40	6	*A*
	3295	5	12	6	*C*
	3273	1	132	8	*A*
	3242	1	88	8	*A*
63′	3220	3	26	6	*A*
	3202	5	14	6	*C*
	3168	1	88	8	*A*
	3150	1	92	8	*A*
66′	3117	1	92	12	*A*
	3104	1	98	12	*A*
	3076	1	80	8	*A*
68′	3058	2	40	8	*A*
	3036	1	154	8	*A*
69′	3013	1	150	8	*A*
70′	2971	2	48	8	*A*
	2948	1	166	10	*A*
71′	2929	2	40	8	*A*
72′	2901	1	41	6	*A*
73′	2873	1	104	10	*A*
74′	2858	2	74	10	*A*
	2841	1	136	10	*A*
	2825	2	72	8	*A*
	2808	1	56	8	*A*
	2779	1	50	8	*A*
	2753	1	134	12	*A*
	2736	1	200	20	*A*
	2723	2	132	20	*A*
78′	2705	1	302	20	*A*
79′	2691	2	114	18	*A*
	2674	3	66	16	*A*
	2661	2	84	18	*A*
	2631	3	30	8	*A*
	2610	2	68	10	*A*
	2592	2	58	10	*A*
	2552	1	64	6	*A*
	2531	1	64	6	*E*
	2505	1	78	6	*E*
	2483	1	70	6	*E*
	2451	2	78	16	*E*
	2438	2	108	12	*E*
	2422	2	92	10	*E*
	2406	1	78	8	*E*
	2387	1	66	8	*E*
	2366	2	46	8	*E*
	2341	2	32	6	*E*
	2331	3	50	12	*E*
	2312	3	80	12	*E*
	2299	3	50	12	*E*
	2282	4	40	10	*E*
	2267	2	80	10	*E*
	2245	2	42	6	*E*
	2228	2	32	7	*E*
	2194	2	40	8	*E*
	2167	1	58	8	*E*
	2130	2	64	10	*E*
	2113	1	96	10	*E*
	2089	2	34	8	*E*
	2070	1	90	10	*E*
	1943	3	14	4	*E*
	1907	2	30	4	*E*
	1864	2	34	6	*E*
	1848	2	28	6	*E*
	1822	1	22	6	*E*
	1787	2	32	6	*E*
	1770	2	32	6	*E*
	1739	2	22	6	*E*
	1720	1	38	6	*E*
	1702	2	26	6	*E*
	1669	1	48	6	*E*
	1647	2	26	6	*E*
	1614	2	20	6	*E*
	1595	2	30	6	*E*
	1542	2	24	6	*E*

TABLE III (*continued*).

Line number	E_γ	$\pm\delta E_\gamma$	I	$\pm\delta I$	Class[c]
	1520	3	16	4	E
	1487	2	30	10	E
	1470	6	12	9	E
	1402	2	20	4	E
	1377	1	24	4	E
	1346	3	10	4	E
	1279	1	30	5	E
	1262	1	55	7	D
	1221	2	20	6	E
	1199	3	10	4	E
	1183	2	25	4	E
	1160	3	10	4	E
	1130	2	20	6	E
	1106	3	15	6	E
	1087	3	15	6	E
	1069	2	20	6	E
	1051	2	15	6	E
	1015	2	15	6	E
	996	3	15	8	E
	982	2	37	8	E
	966	2	30	8	E
	931	2	15	3	E
	912	1	40	4	E
	885	1	34	4	E

[a] Energies in keV. Intensities are observed values in units of counts ×keV.
[b] Line number is given only when correspondence with (d,p) occurs.
[c] Classes; *A*, certain line assigned to $Dy^{164}(n,\gamma)Dy^{165}$ appearing in Fig. 4. *B*, Certain line not assigned to $Dy^{164}(n,\gamma)Dy^{165}$. *C*, Doubtful line. *D*, $C^{12}(n,\gamma)C^{13}$ line. *E*, Unassigned lines.
[d] Absolute intensities in gamma rays per 100 neutrons captured =5.6.
[e] Absolute intensities in gamma rays per 100 neutrons captured =4.3.
[f] Absolute intensities in gamma rays per 100 neutrons captured =0.9.
[g] Absolute intensities in gamma rays per 100 neutrons captured =2.5.
[h] Absolute intensities in gamma rays per 100 neutrons captured =1.1.

to be a single gamma ray is a closely spaced doublet or triplet, then the results listed refer only to the centroid. The observed width of peaks is closely compared to that expected from known single gamma rays found from other targets to insure as much as possible that this does not happen, but it is possible that unresolved doublets are present, especially at the lower energies. The background is assumed to be smooth and is taken to be the sum of a constant plus an exponential.

Using the known radiation width of 150 meV for capture in Dy^{164} and the known level density of 34 eV at the capturing state, the Blatt and Weisskopf estimate for 5-MeV $E1$ transitions from the capturing state is approximately 1% per captured neutron. As shown by Bartholomew,[27] the actual widths for known $E1$ transitions vary by an order of magnitude from this value so that $E1$ transitions might well be as strong as 10%. The strongest observed lines (3′) and (4′), having intensities of about 5%, are almost certainly $E1$ transitions. The three lines (13′), (14′), and (15′) are sufficiently intense so that they could be $E1$ transitions of average strength or $M1$ transitions of somewhat larger strength than previously observed. Since the number of observations of such high-energy transitions in highly deformed nuclei is extremely limited, these transitions must be considered as either $E1$ or $M1$.

[27] G. A. Bartholomew, Ann. Rev. Nucl. Sci. **11**, 259 (1961).

In order to determine the neutron binding energy it is necessary to assume that the ground-state gamma ray is observed or else have some knowledge of the specific excited state to which a transition occurs. Since the even-even nucleus Dy^{164} forms a compound state of spin $\frac{1}{2}$ on capturing a thermal neutron, a direct transition to the known ground state of spin $\frac{7}{2}$ would be an octupole transition and is not expected to be observable. The well-known 1.2-min isomeric state at 108.16 keV has spin $\frac{1}{2}$ and an $E1$ transition should occur from the capturing state. This has been assumed to correspond to the highest strong gamma ray seen in the spectrum, line (3′), at 5606.7 keV. The binding energy is then given by 5606.7+108.16, or approximately 5715 keV. The error associated with this energy is estimated to be 4 keV. Some verification is found from the $C^{12}(n,\gamma)C^{13}$ ground-state transition which is within 1 keV of the expected energy. The Q_0 for the (d,p) reaction is similarly found to be (3380+108.16)=3488 keV. This corresponds to a neutron binding energy of 5713±5 keV, in good agreement with the capture gamma-ray determination. Excitation values for both the (d,p) and (n,γ) spectra are taken relative to the peaks (3) and (3′) assumed to correspond to 108.16 keV.

C. Comparison of the (d,p) and (n,γ) Results

There are great advantages in the comparison of the (d,p) and (n,γ) data. The (n,γ) high-energy transitions selectively excite those states which have spin parity of $\frac{1}{2}\pm$ and $\frac{3}{2}\pm$ from the much larger set of (d,p) excited levels. Furthermore, it is often possible on the basis of gamma-ray intensities to choose between electric and magnetic dipole transitions which then gives a preferred parity. In this section we will compare the (d,p) and (n,γ) spectroscopic results and arrive at a list of levels whose spectroscopic character will be considered in Sec. III.

In Table IV a list of the level energies determined from the (d,p) and high-energy (n,γ) spectra are given. In those cases where these two values are believed to correspond to the same state, a weighted average is given for the best value.

Perhaps the most revealing comparison between the two methods of excitation is shown in Fig. 4. This is a histogram comparing the high-energy gamma-ray transitions with the (d,p) peaks adjusted by the binding energy of the deuteron (2225 keV). It is to be noted that at the highest energies (low excitation of Dy^{165}) the gamma-ray transitions do indeed pick out certain specific levels populated by the (d,p) reaction, but as the energy of the gamma rays decreases by about 1 MeV below the binding energy, the correspondence is much less definite. At about this energy, the high-energy gamma rays can correspond not only to *primary* transitions from the capturing state, but may arise as the

TABLE IV. Dy^{165} levels.

Group number[a]	(d,p)[b] (keV)	(n,γ)[c] keV	Best level value[d]	Group number[a]	(d,p)[b] keV	(n,γ)[c] keV	Best level value[d]
2	84.5			41	1893	1895	1895
3	108.2[a]	108.2[b]	108.2	42	1920		
4	158.4	158.5	158.5	43	1949		
5	180.7			44	1971	1967	1968
				45	2006	2007	2007
7	261.5						
8*A*	296.3			46	2029		
8*B*	303.3			47	2069		
9	336.9			48	2076		
10	360.5			49	2098	2103	2101
				50	2124		
11	480						
12	519			51	2152		
13	537[e]	539.4	539	52	2179	2188[e]	
14	574[e]	572.2	573	53	2209	2214	2212
15	605	605.9	605.5	54	2230	2233	2232
				55	2247		
16	629						
17	658			56	2268	2271	2271
18	707			57	2288	2294	2292
19	773			58	2323	2323	2323
20	884			59	2373		
				60	2432		
21	919						
22	1054			61	2445		
23	1106	1103	1104	62	2459		
24	1145			63	2495	2495	2495
25	1166	1167	1167	64	2524?		
				65	2576		
26	1262						
27	1316			66	2596	2597	2597
28	1343			67	2620		
29	1389			68	2657	2657	2657
30	1407			69	2704	2702	2702
				70	2741	2744	2743
31	1452	1452	1452				
32	1506			71	2792	2786	2789
33	1563	1559	1560	72	2815	2814	2814
34	1598			73	2834	2842	2841
35	1652			74	2859	2857	2858
				75	2899		
36	1700	1697[e]					
37	1725			76	2920		
38	1753	1758	1756	77	2948		
39	1835	1830	1832	78	3006	3010	3009
40	1863			79	3016	3024	

[a] Corresponds to Table I and Fig. 4.
[b] Assumes $Q=3380$ keV corresponds to 108.16-keV level.
[c] Assumes 5606.7-keV γ ray comes from decay of capturing state to 108.16-keV level.
[d] Best value entered only when (n,γ) observed.
[e] Possible doublet.

second gamma ray which is preceded by a lower energy gamma ray. In this latter case, the high-energy gamma ray would not correspond directly to the proton group Q sequence. It is evident from Fig. 4 that there is no correlation between intensities observed by the two methods.

Figure 5 shows the low-lying levels ascribed to Dy^{165} utilizing the data presented above. Those levels that are indicated by a solid line are observed in the (d,p) reaction or both the (d,p) and the (n,γ) reactions. The value for the excitation from the (d,p) reaction is shown on the left side of a level and from the (n,γ) on the right side, when observed. The dashed levels and their energies are inferred from the expected systematics.

III. SPECTROSCOPY OF Dy^{165}

A. Intrinsic Nilsson Orbitals

A detailed spectroscopic description of Dy^{165} must, of necessity, involve a careful analysis of the intrinsic Nilsson states expected at a deformation of ~ 0.3 for neutron orbitals in the vicinity of $N=99$. Neutron orbitals in the deformed region between 82 and 126 are shown in Fig. 6. The precise energy spacing between the intrinsic Nilsson orbitals expected cannot be determined theoretically or empirically. However, an approximation may be obtained from the compilation of Harmatz *et al.*[2]

These systematics suggest the following sequence of

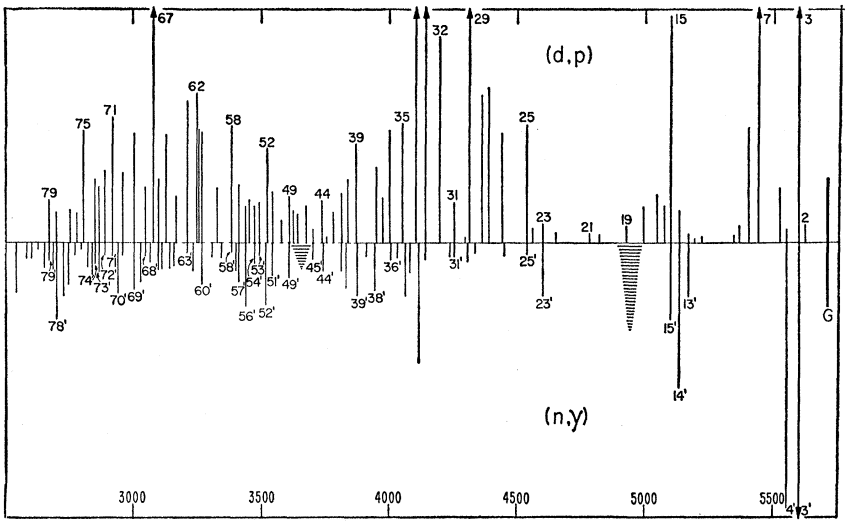

FIG. 4. Bar plot of Q values assigned to $Dy^{164}(d,p)Dy^{165}$ and $Dy^{164}(n,\gamma)$-Dy^{165}, where the (d,p) values have been increased by 2225 keV to allow a more direct comparison. Observed peaks not shown here are given in Tables I and II along with comments explaining their omission. The numbering sequence is chosen to be regular for the (d,p) peaks assigned to Dy^{165}, except for the omission of numbers 1 and 6, but only some of these index numbers are shown. The index number for an (n,γ) peak is shown when it is believed to correspond to a Q value for the (d,p) reaction. The unobserved ground state Q value of 5715 keV is labeled "G." The peaks sketched at 3683 and 4944 keV indicate that the $C^{12}(n,\gamma)C^{13}$ lines obliterate part of the gamma-ray spectrum.

states $(J\pi[Nn_z\Lambda])$: $\frac{7}{2}+[633]$ followed closely by $\frac{1}{2}-[521]$ and $\frac{5}{2}-[512]$ in that order. One might reasonably then expect the $\frac{5}{2}-[523]$ and the $\frac{5}{2}+[642]$ followed by $\frac{3}{2}-[521]$ and $\frac{7}{2}-[514]$. The Nilsson level diagram supports this order in detail with the exception that it reverses the $\frac{7}{2}+[633]$ and $\frac{1}{2}-[521]$ orbitals at a deformation reasonable for Dy^{165}. These tentative assignments have been taken as a starting point in the sections which follow.

B. Intensities in $Dy^{164}(d,p)Dy^{165}$

The differential cross section for the (d,p) stripping reaction has been shown to be a very useful tool for deducing spins in odd-A deformed nuclei.[28] This cross section for a (d,p) reaction on an even-even target nucleus, leaving the residual nucleus in a state of angular momentum I, with Nilsson quantum numbers Ω and N is

$$d\sigma_{I,l,\Omega,N}(\theta)/d\omega = 2C_{I,l}^2(\Omega,N)\phi_l(\theta)U^2, \qquad (1)$$

where l is the orbital angular momentum of the captured neutron, the $C_{j,l}(\Omega,N)$ are normalized coefficients for which $j=I$ for an even-even nucleus of the expansion of the Nilsson wave function $\chi(\Omega,N)$ in a series of wave functions of definite j which are related to the Nilsson coefficients $a_l(\Omega,N)$ by the Clebsch-Gordan transformation

$$C_{j,l}(\Omega,N) = \sum_{\Lambda} a_{l,\Lambda}(\Omega,N)\langle l,\tfrac{1}{2},\Lambda,\Sigma \,|\, I,\Omega\rangle. \qquad (2)$$

The $\phi_l(\theta)$ are intrinsic single-particle cross sections which contain all the angular dependence of the cross section. This is normally calculated using the distorted-wave Born approximation.

These calculations were not available for Dy^{165}. Consequently the intrinsic particle cross section ϕ_l was assumed to be proportional to $2^{-(l+1)}$. This assumption at first sight appears very drastic since it removes all angular dependence. However, at the 12-MeV deuteron bombarding energy used in these experiments and at 45 and 65° for the same proton group the assumption is experimentally verified within a factor of 2 in most cases. The l dependence of the intrinsic particle cross section has been used repeatedly in this and other experiments and normally gives qualitative agreement within a factor of 2.

The U^2 in Eq. (1) is the probability that an orbital in the target nucleus was available for occupation at the time of the reaction. Without pairing correlations it would be zero for all "hole states" and 1.0 for particle states. With pairing correlations, states close to the ground state have a U^2 of $\sim$0.5. In view of the fact that most of the states of interest here are relatively

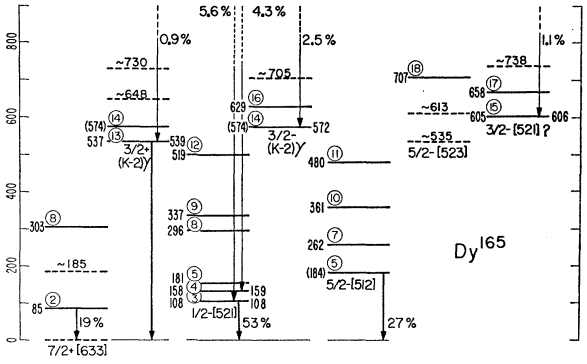

FIG. 5. Proposed level scheme for Dy^{165}. Observed proton peak numbers are circled and the excitation value in keV from the (d,p) reaction is given on the left side of a level when observed. Similarly, the excitation from the (n,γ) reaction is given on the right side when observed. Levels inferred are dashed and the excitation value estimated is discussed in the text. Rotational bands are separated horizontally and only the band head level has the spin and parity shown. The associated levels in each band have a spin increased by one unit from the level below and the same parity.

[28] M. N. Vergnes and R. K. Sheline, Phys. Rev. **132**, 1736 (1963).

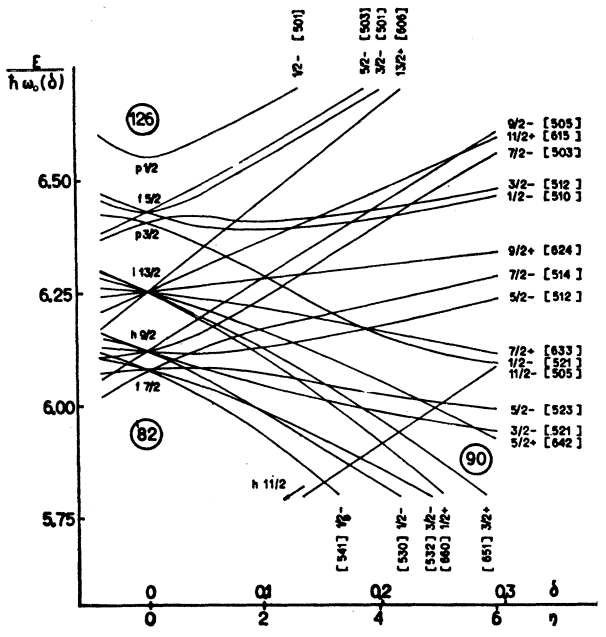

FIG. 6. Nilsson neutron orbitals for deformed nuclei versus deformation as given in Ref. 1.

close to the ground state, U^2 is assumed to be 0.5 for all states.

With these simplifying assumptions it is possible to construct a histogram of the low-lying intrinsic Nilsson states and their associated rotational bands. This is shown in Fig. 7. The measured relative cross sections at 45 and 65° are shown as the bars to the left and right, respectively. The circle is the theoretical value calculated assuming the specific Nilsson orbitals and specific rotational states as shown in Fig. 5. The ability to calculate intensities which differ by as much as two orders of magnitude to within a factor of 2, or in most cases even better, seems to justify the assumptions. The detailed assignment of Nilsson states and their associated rotational bands utilizes the histogram in Fig. 7 in considerable detail. (See Sec. III.C.)

C. Detailed Nilsson Orbital Assignment

Utilizing the (d,p) intensities and the multipolarity assignments from the (n,γ) spectroscopy, it has been possible to assign intrinsic Nilsson states and their associated rotational bands in the low-energy excitation spectrum of Dy^{165}. The reasons for these assignments will be considered separately for each rotational band in turn as it appears in the excitation spectrum.

1. The Ground-state $\frac{7}{2}+[633]$ Band

Transitions directly to the ground state are not observed in either the (d,p) or (n,γ) spectra. This is to be expected because of the low cross section predicted for the (d,p) reaction (see Sec. III.B above), and because in the (n,γ) process the $\frac{1}{2}+$ capture state in Dy^{165} cannot be expected to populate the $\frac{7}{2}+$ ground state directly. Fortunately, the $\frac{1}{2}-[521]$ state is strongly populated by both the (d,p) and (n,γ) mechanisms. Knowing the energy of this $\frac{1}{2}-$ state allows the location of all observed levels relative to the ground state. Built upon the ground-state intrinsic Nilsson orbital ($\frac{7}{2}+[633]$) we then expect the superimposed rotational band members with spins $\frac{9}{2}$, 11/2, 13/2,$\cdots$. We may estimate the moment of inertia parameters from the isotonic nuclei Er^{167} and Yb^{169}. These parameters ($\hbar^2/2\mathcal{I}$) are 8.81 and 7.88 keV, respectively. The population of a weak state (peak 2) at approximately 85 keV in the (d,p) spectrum (moment of inertia parameter of $\sim$9.2 keV) is in approximate agreement with both the expected moment of inertia and the intensity and is therefore assigned as the $\frac{9}{2}+$ first rotational state built on the ground state.

The 13/2+ state is expected to be the most strongly excited in the (d,p) reaction of all the members of the rotational band built on the $\frac{7}{2}+[633]$ orbital. Utilizing the moment of inertia determined from the $\frac{7}{2}+$—$\frac{9}{2}+$ energy difference, the 13/2+ state is predicted with reasonable rotation-vibration interaction correction to lie at 304 keV. The upper member of the doublet at $\sim$300 keV agrees in intensity and in energy with this assignment. The position of the 11/2+ is then calculated as $\sim$185 keV. It should not be populated directly in the (n,γ) spectrum, and the cross section for its production in the (d,p) reaction is so small that it cannot hope to be observed in the presence of the strong line at 181 keV. The experimental observation of only the $\frac{9}{2}+$ and the 13/2+ members of the $\frac{7}{2}+[633]$ rotational band in the (d,p) reaction is in agreement with the predicted intensities (Sec. III.B and Fig. 7).

2. The $\frac{1}{2}-[521]$ Band

The position of the $\frac{1}{2}-[521]$ band 108.16 keV above the ground state is clearly indicated both by the strongest high-energy direct γ transition from the capturing state (3′) and by an extremely strong (d,p)

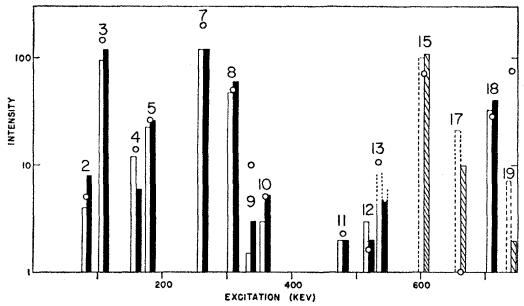

FIG. 7. Bar plot of observed and estimated relative intensities for the (d,p) reaction. The numbers refer to the proton group number as shown in Fig. 5. The left bar is the observed 45° intensity and the right bar the 65° intensity. The circles are the calculated intensities as described in Sec. III.B.

proton group (3). The $\frac{3}{2}-$ rotational state built on this band is also evident in both the high-energy capture γ spectrum, line (4′), and as a relatively weak proton group (4) from the (d,p) reaction. Comparison (see Fig. 7) between the experimental intensities from the proton groups (4), (5), (8), (9), and (12) with the predicted intensities indicates that we have also observed the rotational members, $\frac{5}{2}-$, $\frac{7}{2}-$, $\frac{9}{2}-$, and $11/2-$ in the (d,p) reaction. Utilizing the energies of the first four members of the $\frac{1}{2}-[521]$ band as derived from the data of Schult *et al.*,[29] it is possible to compute the rotational constants as $\hbar^2/2\mathcal{I}=10.665$ keV, $B=-4.05$ eV, and $a=0.579$. These constants may be compared with the values for this band in a number of other nuclei. Since the decoupling parameter a is given by

$$a=-\sum_{jl} C_{jl}^2(-1)^{(j+1)}(j+1),$$

it depends in a crucial way on the wave function of the intrinsic state and therefore, its variation from nucleus to nucleus is of considerable interest. In order to show this clearly, Harmatz *et al.*[2] have plotted both the decoupling parameter a and the inertial energy parameter $(3\hbar^2/\mathcal{I})$ against the mass number A. If we enter the values for Dy^{165} calculated in this work on their plot, the correlation is no longer satisfactory. This might have been anticipated since the parameters a and $3\hbar^2/\mathcal{I}$ are functions of both neutron and proton number rather than the mass number A. When there are only a few values for the parameters, it is reasonable to plot against A, but as the number of values for a and $3\hbar^2/\mathcal{I}$ increase, it is then preferable and even necessary to plot against both neutron and proton number. This has been done in Fig. 8, where the proton number may be considered as the contour lines and are labeled as such. The values of a and $3\hbar^2/\mathcal{I}$ for Dy^{165} fit well into this plot. It is apparent that both the moment of inertia and the decoupling parameter vary in a complex way with both neutron number and proton number, but are correlated with each other.

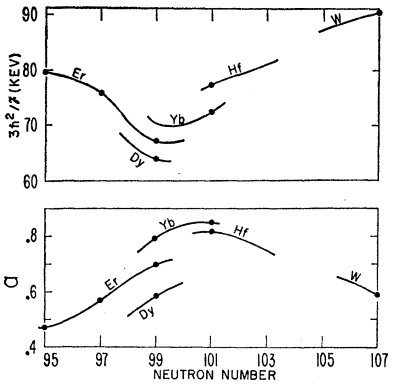

FIG. 8. Plot of the parameter $(3\hbar^2/\mathcal{I})$ and the decoupling parameter a versus the neutron number for the $\frac{1}{2}-[521]$ band. The various isotopes are indicated as contour lines on the diagram.

3. *The Anomaly of the 262-keV State; the $\frac{5}{2}-[512]$ Band*

The $\frac{7}{2}+[633]$ band and the $\frac{1}{2}-[521]$ band together exhaust all of the strong proton groups in the (d,p) spectrum up to 500 keV except the proton group (7) populating the 262-keV state (see Table IV). Because of its strength, this proton group must necessarily belong to the Dy^{165} level structure. The situation is further complicated by the fact that there is a correspondence between a weak neutron-capture γ ray of 5453 keV suggesting spin parity $\frac{1}{2}\pm$ or $\frac{3}{2}\pm$ and peak 7 to this level in the (d,p) spectrum. A search for possible intrinsic Nilsson states indicates only one possibility with spin $(\frac{1}{2},\frac{3}{2})\pm$ which can give such a coincidence, namely, the $\frac{1}{2}+[651]$ intrinsic state. However, there are two serious difficulties with this explanation. In the first place, one would expect to see in the high-energy (n,γ) spectrum transitions going to both the $\frac{1}{2}+$ state and the $\frac{3}{2}+$ rotational state and this latter transition is not seen. In the second place, one would expect to see in the (d,p) spectrum strong populations—both the $\frac{3}{2}+$ and $\frac{5}{2}+$ members of the $\frac{1}{2}+[651]$ rotational band and these proton groups are not seen. It is necessary, therefore, to discard this explanation for the 262-keV state. The most reasonable explanation is that the high-energy gamma ray in the (n,γ) spectroscopy results from $Dy^{163}(n,\gamma)Dy^{164}$ to a known state in Dy^{164}. We are then allowed the possibility of explaining the 262-keV state in terms of other Nilsson orbitals not possessing spin $\frac{1}{2}$ or $\frac{3}{2}$. The $\frac{7}{2}-$ rotational member of the $\frac{5}{2}-[512]$ band is expected to be strongly populated in a (d,p) reaction. Furthermore, there are weaker peaks at 360 and 480 keV in the proton spectrum which correspond well to the $\frac{9}{2}-$ and $11/2-$ members of the band. Finally, there is strong evidence for a state at $\sim$184 keV which should be the $\frac{5}{2}-$ band head. This evidence is in the form of an extremely strong 184-keV γ transition which has been observed by several experimenters (see Sec. II). At first glance, one might assume that the 184-keV transition is from the 181-keV $\frac{5}{2}-$ rotational member of the $\frac{1}{2}-[521]$ band to the ground state. However, this is a $K-$ forbidden transition which cannot possibly compete with depopulation to the lower energy members of the rotational band. Consequently, the 184-keV transition is assigned as an $E1$ transition from the $\frac{5}{2}-[512]$ band head to the ground state. The population of the $\frac{5}{2}-[512]$ level in the (d,p) reaction is weak and is hidden by the strong population of the $\frac{5}{2}-$ member of the $\frac{1}{2}-[521]$ band at 181 keV.

4. *The Triplet of High-Energy Transitions in the (n,γ) Spectrum*

One of the most interesting features of the high-energy (n,γ) spectra is the existence of a triplet of transitions (13′), (14′), and (15′) which correspond to the peaks (13), (14), and (15) observed in (d,p) reaction

[29] These energy values for the $\frac{1}{2}-[521]$ band are: $108.16(\frac{1}{2}-)$, $158.59(\frac{3}{2}-)$, $180.93(\frac{5}{2}-)$, and $297.70(\frac{7}{2}-)$ keV.

spectroscopy and excitations of 539, 573, and 606 keV, respectively. The (n,γ) intensities demand that these be dipole transitions and, therefore, that these states have spin parity $\frac{1}{2}\pm$ or $\frac{3}{2}\pm$. The only Nilsson orbitals available for these spins and parities are the $\frac{3}{2}-[521]$ and the $\frac{1}{2}-[510]$ orbitals. However, the systematics of the position of these orbitals relative to the position of the $\frac{7}{2}+$ ground state indicate that, although the $\frac{3}{2}-[521]$ orbital is to be expected in the region from 500 to 600 keV, the $\frac{1}{2}-[510]$ orbital normally is expected $\sim$1300 keV above the ground state. If one assumes that the $\frac{1}{2}-[510]$ orbital is seriously displaced in energy, it is possible to get an approximate fit of the energies in this region into two rotational bands—a $\frac{3}{2}-$ and $\frac{1}{2}-$ band—utilizing the (d,p) levels observed. However, in addition to the serious $\frac{1}{2}-$ band energy anomaly, there are states left over which do not fit into any reasonable rotational pattern. Furthermore, the intensities of the proton groups resulting from the $\frac{1}{2}-[510]$ rotational band are in serious disagreement with the theoretical predictions. An alternative interpretation involves three rotational bands, two of which are the gamma vibrational bands built on the $\frac{7}{2}+[633]$ and $\frac{1}{2}-[521]$ intrinsic states. The third band is built on the intrinsic state $\frac{3}{2}-[521]$. This interpretation is not unreasonable because (a) the energy of the gamma vibrational bands above the intrinsic states on which they are built is in agreement with systematics (see Sec. IV) and (b) the moments of inertia of the gamma bands are very similar to those of the intrinsic states on which they are built.

In the sections which follow, it will be shown in considerably greater detail that this interpretation is much more consistent with the data than the interpretation utilizing the $\frac{1}{2}-[510]$ intrinsic configuration.

5. *The Postulated $\frac{3}{2}+$ γ Vibrational Band at 538 keV*

The level at 539 keV corresponding to proton group (13) has unique population and decay characteristics. There is a relatively strong 5175-keV γ-ray transition (13′) feeding this state directly from the capturing state and a strong gamma-ray transition[20] that very likely accounts for depopulating it directly to the ground state. This decay sequence fits the energies correctly and has been observed in a coincidence experiment by Neill.[30] This is probably the only observable prompt two-step cascade to the ground state. Only a fast $M1$ transition from the capturing state and a fast $E2$ transition to the ground state can explain such a strong two-step decay mode. This suggests that the spin of this state is $\frac{3}{2}+$ and gives a number of clues to its character. The only reasonable interpretation is that it is the $\frac{3}{2}+$ γ band built on the $\frac{7}{2}+[633]$ ground state. The fast 539-keV $E2$ transition to the intrinsic state on which the γ vibration is built is expected. Such a vibrational band should have a moment of inertia very close to that of the intrinsic state on which it is built. If the moment of inertia of the $\frac{7}{2}+[633]$ band is assumed, the following states are predicted: $\frac{5}{2}+$ at 584 keV, $\frac{7}{2}+$ at 648 keV, and $\frac{9}{2}+$ at 730 keV. The energies of the predicted $\frac{5}{2}+$, $\frac{7}{2}+$, and $\frac{9}{2}+$ states are close enough to those of the proton groups (14), (17), and (19) at 574, 658, and 738 keV to have been masked particularly if they are weak. Since there is no theoretical prediction of (d,p) cross sections to gamma vibrational bands, it is not possible to use the observed intensities. This points, however, to the need for this type of prediction.

6. *The Postulated $\frac{3}{2}-$ γ Vibrational Band at 574 keV*

A moderately weak proton group, (14), is observed populating a state at 574 keV in Dy^{165}. This state is directly and strongly populated by an $E1$ transition from the neutron capture state. This suggests spin $\frac{1}{2}-$ or $\frac{3}{2}-$ for the 574-keV state. Reasonable assignments are a γ vibrational band built on the $\frac{1}{2}-[521]$ intrinsic state or a $\frac{3}{2}-[521]$ intrinsic state. Since there is a higher energy state at 629 keV which may reasonably be expected to be the first rotational member of this band, and since the moment of inertia which this energy difference gives is very similar to that of the $\frac{1}{2}-[521]$ band, it is assumed that this is the γ vibrational band. Using this moment of inertia, one computes a state at $\sim$705 keV very close to (the strongly populated state) experimentally observed at 707 keV which would mask it.

7. *The $\frac{3}{2}-[521]$ Rotational Band*

There is an extremely strong proton group to a state at 605 keV corresponding to group (15) and high-energy γ ray (15′). This state is tentatively assigned as the $\frac{3}{2}-[521]$ intrinsic state. States at 658 keV, (17), and 738 keV fit approximately into a rotational band. The latter state, which falls between groups (18) and (19), is not listed in Table I because the data are not sufficiently certain. There are difficulties with this interpretation, however. The (d,p) population of the $\frac{5}{2}-$ rotational state is expected theoretically to be weaker than experimentally observed (see Fig. 7). Coriolis mixing of this $\frac{5}{2}-$ state with other known near-lying $\frac{5}{2}-$ states (for example, the $\frac{5}{2}-$ or the γ vibrational band and the $\frac{5}{2}-[523]$: see Sec. III.C.8, which follows) might increase the expected intensity considerably. However, the $\frac{5}{2}-$ states with which mixing is expected are themselves weak. Furthermore, the experimental intensity of the proton group populating the 738-keV state with proposed spin parity $\frac{7}{2}-$ is too weak. In view of the good qualitative agreement between (d,p) intensities in experiment and theory shown in Fig. 7, these two discrepancies are serious. Consequently, the interpretation in terms of the $\frac{3}{2}-$ band must be considered tentative.

[30] J. M. Neill, thesis, MIT, September 1963 (unpublished).

8. The Anomaly of the 707-keV State; the $\frac{5}{2}-[523]$ Band

The three bands discussed in III.C.5, 6, and 7 exhaust all of the experimentally observed states in the energy region from 500 to 750 keV except the 707-keV state, corresponding to group (18). The most reasonable candidate for a state strongly populated by (d,p) is the $\frac{9}{2}-$ state built on the $\frac{5}{2}-[523]$ intrinsic state. This assumption and the known moment of inertia for the $\frac{5}{2}-[523]$ band in Dy^{163} and Er^{168} suggest the existence of states at 533 and 613 keV. The slight disagreement between the state suggested by the capture γ transition and that populated by the (d,p) reaction (539 and 537 keV, respectively) may result because the proton group shows the presence of states at both 533 and 539 keV, whereas the (n,γ) transition goes only to the 539-keV level. If one assumes arbitrarily equal intensities for the population of the two states by (d,p) reaction, the energy for the $\frac{5}{2}-[523]$ band head would be 535 keV. This is the energy suggested in Fig. 5. The $\frac{7}{2}-$ rotational level at 613 keV would surely be lost in the strong 605-keV proton group. Thus, although only one state has been seen with certainty in this band, the intensity of this state makes it probable that the Nilsson assignment is correct.

9. Brief Description of the High-Lying Levels

A relatively large number of intrinsic Nilsson states have been observed in Dy^{165}. However, even more should exist in the low-energy excitation spectrum. To be expected are the following intrinsic states and their associated rotational bands: Somewhere in the region immediately above the $\frac{5}{2}-[523]$ state one expects to observe the $\frac{5}{2}+[642]$ state. Probably only the $\frac{9}{2}+$ and 13/2+ members of this band will be seen in (d,p) reaction spectroscopy because of the expected intensities. In addition, the $\frac{9}{2}-$ member of the $\frac{7}{2}-[514]$ band and the 13/2+ member of the $\frac{9}{2}+[624]$ band are to be expected at somewhat higher excitation energy but below 1 MeV. The $\frac{1}{2}+$ and $\frac{3}{2}+$ members of the rotational bands built upon the $\frac{1}{2}+[660]$ and the $\frac{1}{2}+[651]$ states should be directly populated by high-energy transitions in the capture gamma-ray spectrum. These cannot, however, be positively identified. It would be particularly interesting to locate the $\frac{1}{2}+[651]$ band since it originates from the shell above.

The $K+2$ counterparts of the $K-2$ γ-vibrational bands already observed may be expected to lie 100–200 keV above the K-2 bands already described. The low-intensity "hash" in the vicinity of groups 20 and 21 may represent an extremely complex mixture of the low-intensity states just described. The $K-2$ γ-vibrational band built upon the $\frac{5}{2}-[512]$ state has not been assigned but should be at around 600-keV excitation. Both the $\frac{1}{2}-$ and $\frac{3}{2}-$ members should be directly excited in the capture spectrum.

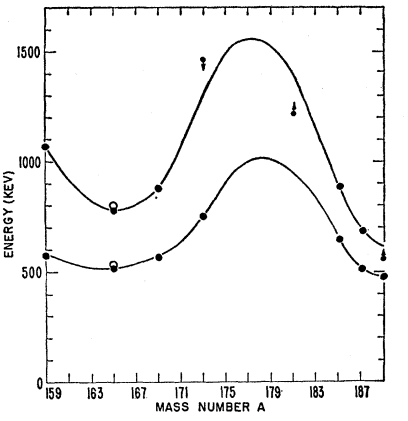

FIG. 9. Energies of the $K-2$ γ-vibrational bands above their intrinsic parent levels. Upper curve: solid points are the average energies of neighboring even-even nuclei. Lower curve: solid points are the energies of vibrational bands built on odd proton orbitals. See Sec. IV. A of text for further details.

IV. VIBRATIONAL STATES IN ODD-A NUCLEI

A. Energy Systematics of $K-2$ Gamma Vibrations of Odd-A Nuclei

There are two gamma-vibrational bands built on each intrinsic Nilsson state of an odd-A nucleus. These are the $K-2$ and $K+2$ vibrations. There are beginning to be enough $K-2$ vibrations to look for energy systematics. However, fewer $K+2$ species have been observed and the uncertainty involved in the tentative observation of these species is much greater in general. In view of the fact that this research postulates the first gamma vibrations built on intrinsic Nilsson states involving neutrons, a survey of the systematics of all gamma vibrations was undertaken. Of special interest are (1) the energy systematics of the $K-2$ gamma bands relative to the gamma bands of neighboring even-even nuclei; (2) a comparison of the energy of $K-2$ gamma bands built on proton orbitals with those built on neighboring

TABLE V. Compilation of γ vibrations in deformed odd-A nuclei.

Nucleus	Orbital	Energy of $K-2$ band (keV)[a]	Energy of $K+2$ band (keV)	ΔE[b]
Tb^{159}	$\frac{3}{2}+[411]$	580	(1280)	(700)
Dy^{165}	$\frac{7}{2}+[633]$[c]	539		
Dy^{165}	$\frac{1}{2}-[521]$[c]	465		
Ho^{165}	$\frac{7}{2}-[523]$	515	687	172
Tm^{169}	$\frac{1}{2}+[411]$	570	(1170)	(600)
Lu^{173}	$\frac{7}{2}+[404]$	(759)		
Re^{185}	$\frac{5}{2}+[402]$	646	(750)	(104)
Re^{187}	$\frac{5}{2}+[402]$	511	(880)	(369)
Re^{187}	$\frac{9}{2}-[514]$	480		

[a] Energies of bands are taken above the orbital with which they are associated. Parentheses around the energy indicate uncertainties about assignment.
[b] ΔE = Energy difference between $K+2$ and $K-2$ bands in keV.
[c] Neutron intrinsic states on which γ bands are built.

TABLE VI. Nilsson orbital assignments for 97, 99, 101, and 103 isotonic species.[a]

Nucleus	$\frac{3}{2}+[651]$	$\frac{3}{2}-[521]$	$\frac{5}{2}+[642]$	$\frac{5}{2}-[523]$	$\frac{7}{2}+[633]$	$\frac{1}{2}-[521]$	$\frac{5}{2}-[512]$	$\frac{7}{2}-[514]$	$\frac{9}{2}-[624]$
Dy^{163}				0					
Er^{165}	((853))	(242)	(47)	0	((117))	(297)	(608)		
Yb^{167}		((239))	(29)	(0)					
Dy^{165}		((606))		535	0	108	184		
Er^{167}				((585))	0	207	((347))		
Yb^{169}				(570)	0	(24)	(191)	((962))	
Yb^{171}					(95)	0	122	(835)	936
Hf^{173}						0	((107))		
Yb^{173}					351		0	636	
Hf^{175}					(207)	125	0	(348)	

[a] Single and double parentheses indicate decreasing certainty.

neutron orbitals, and (3) a survey of the energy differences between $K-2$ and $K+2$ vibrational bands to understand the nature of this splitting. The available data are shown in Table V.

A comparison between the energy systematics of the $K-2$ γ vibrational bands and the γ bands of neighboring even-even nuclei is shown in Fig. 9. In this plot the upper curve is the average of the energy of the γ-vibrational bands of the two even-even nuclei which have one proton more and one proton less than the odd-A nucleus under consideration. For example, the Tb^{159} γ vibration is compared with average of the vibrations in Dy^{160} and Gd^{158}; the Ho^{165} with Er^{166} and Dy^{164}. In certain cases one of the two gamma-vibrational energies was unavailable for the average. In these cases the systematics tells us what direction the effect of having the additional gamma vibration will push the average. This is indicated in the figure by an arrow. The lower curve is a plot of the $K-2$ gamma-vibrational bands built on proton orbitals.

It is apparent that the two curves "mirror" each other to a striking extent. In view of this fact, it should be possible to approximately predict the energy of other $K-2$ γ vibrational bands. Thus, for example, it seems probable that a second smaller maximum in the energy systematics will occur in the region $A=155$–157.

Another interesting comparison also emerges from Fig. 9. The two hollow circles at mass 165 represent on the lower curve the energy of the $K-2$ γ vibration built on $\frac{7}{2}+[633]$ *neutron* orbital and on the upper curve the average of the vibrational energies for Er^{166} and Er^{168}. It therefore seems possible that $K-2$ γ band systematics of odd-neutron orbitals will be almost identical to those of the odd-proton orbitals and will also approximately mirror the appropriate even-even nuclei.

V. CONCLUSION

A large number of intrinsic states and γ-vibrational states have been observed in the low-energy excitation spectrum of Dy^{165}. The states observed are consistent with the Nilsson intrinsic states expected in this region of odd-A neutron orbitals as shown in Table VI. Built on the two lowest intrinsic states are $K-2$ γ-vibrational bands. It is particularly interesting to note that the calculated moments of inertia of the postulated γ-vibrational bands are close to those of the intrinsic states on which they are built, and that the rotational constants of the postulated intrinsic states are similar to those observed in other nuclei. A brief analysis of vibrational bands in odd-A nuclei indicates an excellent correlation between γ-vibrational bands in odd-A nuclei and γ-vibrational bands in corresponding even-even nuclei.

It has been clearly demonstrated that (d,p) reaction spectroscopy and neutron-capture γ-ray spectroscopy are successful complimentary methods of studying the complex low-energy excitation spectra of deformed odd-A nuclei and lead in this case to several assignments up to 0.7 MeV. It is clear that additional intrinsic states and γ-vibrational states and their superimposed rotational bands are present in the Dy^{165} level spectrum below 1 MeV. High-resolution low-energy γ-ray experiments with bent crystals and internal conversion measurements would bring to bear additional experimental information on this obviously complex problem. Such data should confirm the assignments suggested by the present data and it appears from an initial perusal that the low-energy capture gamma-ray data obtained at Risø[20] fit well into the scheme shown in Fig. 5. A detailed analysis of this data will be published in the near future.[20] Only a small amount of the data obtained in both the (d,p) and (n,γ) reactions has been utilized in the present analysis and confirmation of the level scheme up to 700 keV should permit further use of the data to higher energies.

It seems evident that the collaboration by workers using different instruments and techniques is essential in the development and understanding of the level structures of deformed odd-A nuclei. The techniques now available have reached a standard that promises to allow reasonably complete level schemes to be obtained in many cases.

ACKNOWLEDGMENTS

We wish to thank the staff of the Tandem Van de Graaff at Florida State University and the plate counters under the direction of Mary Jones and also the operating staff of the Los Alamos Omega West Reactor. Helpful critical discussions were held with Dr. Authur Kerman and Dr. M. E. Bunker. The assistance of Dr. E. T. Jurney, Parvin Lippincott and Mrs. K. H. Harper is gratefully acknowledged. We are especially indebted to Dr. O. W. B. Schult and his coworkers for allowing us to quote the low-energy capture data prior to its publication.

PHYSICAL REVIEW VOLUME 136, NUMBER 2B 26 OCTOBER 1964

Decay of Xe^{137} †

RONALD J. ONEGA* AND WILLIAM W. PRATT
Department of Physics, The Pennsylvania State University, University Park, Pennsylvania
(Received 10 June 1964)

The decay of Xe^{137} was studied by means of scintillation techniques. The radioactive samples were produced by means of neutron irradiation of natural xenon, which contains 8.87% Xe^{136}. The half-life of Xe^{137} was found to be 3.95±0.11 min. One gamma ray of 0.455±0.003 MeV was attributed to Xe^{137}. An upper limit of 0.03 of the intensity of this gamma ray is placed on any other gamma ray due to the decay of Xe^{137}. The end-point energy of the beta spectrum was found to be 4.06±0.06 MeV using K^{42} as a calibration check. A beta ray was found to be in coincidence with the 0.46-MeV gamma ray. A Kurie plot of the beta-gamma coincidence spectrum as well as a subtraction method of the singles Kurie plot were both in agreement with 3.60±0.06 MeV for the lower-energy beta group. In order to get the intensity of the two beta transitions, two independent methods were utilized. These indicated a relative intensity of about 0.33±0.03 for the 3.60-MeV beta-ray group and 0.67±0.03 for the 4.06-MeV beta-ray group. Log*ft* values indicate first-forbidden beta-ray selection rules for both transitions. This is found to be in accord with shell-model predictions. A decay scheme is proposed on the basis of these results.

I. INTRODUCTION

THE beta-ray spectrum associated with the 3.9-min activity of Xe^{137} has previously been studied by absorption techniques.[1,2] Energies of 4 MeV[1] and 3.5 MeV[2] were reported. The gamma-ray spectrum has been investigated using scintillation techniques.[3,4] A gamma ray of 0.44 MeV was reported which decayed with a half-life of about four minutes and which was attributed to the decay of Xe^{137}. The work reported here was undertaken in order to obtain a more definitive study of the beta-ray spectrum, to search for additional gamma rays, and to relate the decay scheme of Xe^{137} to the energy level structure of Cs^{137}.

II. EXPERIMENTAL PROCEDURE

In the present investigation sources were prepared by irradiating natural xenon gas in the Pennsylvania State University Research Reactor. The procedure for handling the gas from the shipping container was as follows: Displace about half of the water in a 50-ml polyethylene bottle with xenon gas; expose the sample of gas in the reactor; transfer the irradiated gas from the polyethylene exposure bottle to a counting cell. The counting cell was an aluminum cylinder with a polyethylene window approximately 1 mil thick.

Beta- and gamma-ray spectra were studied using conventional methods of scintillation spectroscopy. A 3-×3-in. NaI(Tl) crystal was used for measuring the gamma-ray spectra and was also used in conjunction with a 2-×2-in. NaI(Tl) crystal for coincidence measurements. A 2-×2-in. anthracene crystal was used for the beta-ray measurements. Beta-gamma coincidence measurements employed the 3-in. NaI(Tl) crystal and

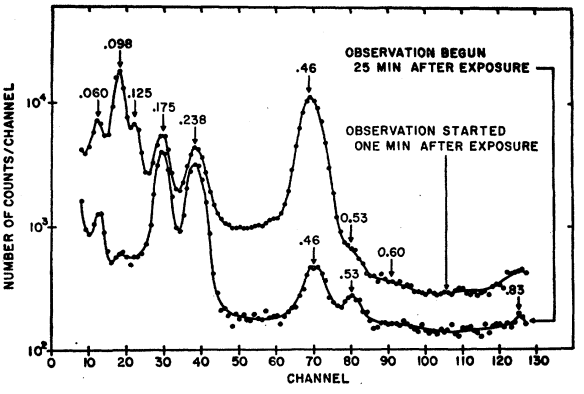

FIG. 1. Xe^{137} gamma-ray spectrum for energies less than 0.85 MeV; observations 24 min apart.

† This work was supported in part by the U. S. Atomic Energy Commission.
* Present address: Department of Physics, Virginia Polytechnic Institute, Blacksburg, Virginia.
[1] H. Born and W. Seelmann-Eggebert, Naturwiss. **31**, 201 (1943).
[2] S. Nassiff and W. Seelmann-Eggebert, Z. Naturforsch. **10a**, 83 (1955).
[3] S. Prakash, Z. Elektrochem. **64**, 1037 (1960).
[4] D. W. Ockenden and R. H. Tomlinson, Can. J. Chem. **40**, 1594 (1962).